Synthesis and characterization of barium hexaferrite ($BaFe_{12}O_{19}$) nanoparticles from iron ore waste and their possible application in water treatment

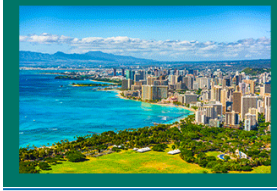

IOP Conf. Series: Materials Science and Engineering **975** (2020) 012002 doi:10.1088/1757-899X/975/1/012002

Synthesis and characterization of barium hexaferrite ($BaFe_{12}O_{19}$) nanoparticles from iron ore waste and their possible application in water treatment

Nehal A. Erfan[*a], **Salwa A. M. Abdel-Hameed**[b], **Asma A. Mohammed**[a]

[a] Chemical engineering department, faculty of engineering, Minia university, Minia, Egypt.
[b] Glass Research Department, National Research Centre, Dokki, Cairo, Egypt
Email: n.erfan1@mu.edu.eg

Abstract. In this work hard magnetic glass ceramics has been fabricated using Egyptian Bahariya oasis ore; which contains not less than 51% of its weight as pure iron. High energy planetary ball mill was used to convert the prepared magnetic sample into nanoparticles. Different mechanical milling times were applied to study its effect on the properties of the produced magnetic glass ceramic. Scanning electron microscope (SEM), transmission electron microscope (TEM), X-ray florescence analysis (XRF), differential thermal analysis (DTA), X-ray diffraction analysis (XRD), Raman spectroscopy and Vibrating sample magnetometer (VSM) analysis techniques were performed to characterize the prepared glass ceramic samples before and after exposing to mechanical milling process. XRD revealed crystallization of barium hexaferrite as major phase with average crystallite size ~26 nm. Saturation magnetization Ms depicted 21.2 emu/g after 5 hours milling. The produces nanoparticles after 5 hours milling showed a good performance in removal of pollutants like methylene blue and Congo red from water by adsorption.
Key words
Magnetic glass ceramics; Ball milling; Barium hexaferrite; nanoparticles;Iron ore, Waste; Recycling

1. Introduction

East Aswan, Eastern desert, Bahariya oasis and Western desert are localities rich with iron ore mines in Egypt. In these localities, the iron ore deposits widely and vary in their chemical and mineralogical composition. In this work Bahariya oasis ore which contains not less than 51% of its weight as pure iron has been used for preparing magnetic glass ceramics. Huge amount of iron ore is wasted during ore extraction, tailing removal, crushing, grinding and screening processes; as pretreatment steps to reach the suitable size for blast furnace use. Not less than 20% of iron oxide from iron ore is wasted. This iron oxide waste could be used as raw material for magnetic glass ceramics production [1]. Hard ferrites or permanent magnets are viewed as important material for different engineering applications. It characterized by its high coercivity, remanence after magnetization, high magnetic permeability and the ability to conduct magnetic flux. Ferrite magnets are widely used compared to other magnets as metallic alloys because of their low cost. Hard ferrite magnets have a wide variety of applications such as refrigerator magnets,electric motors, magnetic separators for ferrous materials, automotive sensors, MRI,

microwave devices, wireless communications, data storage and air crafts as well as many other novel applications.

An increasing interest in hexaferrite nano-fibers and the effect of fiberous structure on magnetic properties is grown recently. On the other hands, ferro-fluid technology is one of the important applications for magnetic nanoparticles. Nano-ferro-fluids have many biomedical applications, for example, hyperthermia treatment for cancer [1], MRI contrast agent [2], drug delivery [3], DNA hyberdization [4] and cell separation [5].Nano-ferrites and a different iron-containing minerals (akaganeite, feroxyhyte, ferrihydrite, goethite, hematite, lepidocrocite, maghemite, and magnetite [6]were used for waste water treatment.The produced magnetic nanoparticles can be added to a polymer solution prior to electrospinning for synthesis magnetic nanofibers by ex-situ approach [7]. Magnetic nanofibers have a wide range of applications in biomedical engineering [8], tissue engineering [9] and waste water treatment [10, 11].

Since the very early development of nanoscience, creating nanomaterials using simple and low cost techniques with high yield was a great challenge. High energy ball milling technique has been used widely for nanomaterials, nanograins, nanoalloy, nanocomposites and nano-quasicrystalline materials synthesis. During milling process the energy transferred from the balls to the powder which control the kinetics of alloying [12].Type of mill, kind of powder, milling speed, size of balls, wet or dry milling, milling temperature and milling duration are the main parameters govern the energy transfer from balls to milled powder [13]. Dense materials (steel or tungsten carbide) are preferable to ceramic balls because the kinetic energy of the balls is a function of their mass and velocity, in addition, the size and size distribution are optimized for the given mill [14]. Dilute distribution of the milling balls minimizes the collision frequency, while too dense packing of balls reduces the mean free path of the ball motion [15].
Material characteristic of the powder and milling media and the kinetic energy of the ball were the factors affecting temperature during milling process.Also, defect concentration and diffusivity of the milled powder are very sensitive to temperature which influences the phase transformations induced by milling [16]. The formation of phases which need higher atomic mobility (intermetallics) is induced by higher temperatures while, amorphous and nanocrystalline phases formation take place at lower temperatures [17, 18].

Particle size reduction, mixing, particle shape changes and synthesis of nanocomposites are the main objectives of mechanical milling. High energy ball mill is the typical mill used for these purposes such as vibratory mills, tumbler ball mills, planetary mills, and attritor mills etc. The internal mechanics of the specific mill, the power supplied to drive the milling chamber; the composition, size, and size distribution of the balls influence the energy of the milling media. Ball mass-to-powder mass ratios of 5 to 10 are typically used and are effective. Various industrial processes use synthetic chemical dyes over the last few years. Paper and pulp manufacturing, plastics, dyeing of cloth, leather treatment, printing are examples of the areas where these chemicals are frequently used. Industrial waste waters containing such dyes are generally considered as effluents. Because of the toxicity of some of these dyes, their removal from industrial effluents can be a major environmental problem [19, 20]. The highly colored waste water in the presence of various dyes block sunlight and oxygen penetration which are both vital for various forms of aquatic life. Moreover, carcinogenic compounds which end up in food chain can be formed as the dye solution undergo anaerobic degradation [21]. From an environmental and economic point of view, removal of dyes from waste water is of significant importance. To remove dyes from aqueous solutions, several methods have been used [22-25]. Among these methods, adsorption is efficient and economical for the removal of dyes from aqueous solutions. Traditional approaches for water treatment, such as chemical precipitation, electrochemical degradation, acidification, biological degradation, activated carbon adsorption and ozone oxidation are generally restricted because of high operating cost, sensitivity to treatment conditions and low efficiency. Using the characteristic of high separation efficiency of magnetic

nanoparticles, the detection and separation of the toxic components of waste water can effectively shorten the working hours and reduce the workload. The novelty of this study is two-fold: first,
Using Baharaiya oasis iron ore for hard ferrimagnetic glass ceramics nanoparticles preparation; second, it provides an assessment of the adsorption efficiency of the proposed nanoparticles.

2. Experimental methods

2.1 Preparation of the glass

Table 1 represents the X-ray fluorescence analysis (XRF) of IOW (iron ore waste) sample. In this works, the prepared samples composition based on $BaFe_{12}O_{19}$ as hard magnet. Table 2 illustrates the composition of the prepared samples. IOH is referred to hard magnetic glass ceramics with composition of ~37% IOW beside Na_2CO_3, $NH_4H_2PO_4$, $BaCO_3$, H_3BO_3 and TiO_2as a source for Na_2O,P_2O_5, BaO, B_2O_3 and TiO_2 respectively.

Platinum crucibles were used to melt the required amounts of chemicals with composition shown in Table 2 at 1200^{o}C. An electrically heated furnace was used for the melting process which lasted for 2 h with occasional swirling every 30 min. to ensure homogenization.The melts were poured onto a stainless steel plate and pressed into 1-2 mm thick strips by another cold steel plate at room temperature. In order to investigate the effect of heat treatment on the phase transformations and sample properties, the produced strips were heat treated at 900^{o}C for 2 h.

Table 1. Quantitative XRF analysis of iron ore waste (IOW)

Constituents	**SiO_2**	**TiO_2**	**Al_2O_3**	**Fe_2O_3tot**	**MgO**	**CaO**	**Na_2O**	**K_2O**	**P_2O_5**	**CuO**	**Cr_2O_3**	MnO	
IOW (wt%)	7.96	0.28	2.79	67.15	0.31	3.96	1.53	0.28	0.48	-	0.028	1.2	
Constituents	**PbO**	**ZnO**	**NiO**	**As_2O_3**	**BaO**	**V_2O_5**	**SrO**	**ZrO_2**	**Y_2O_3**	**Co_3O_4**	**SO_3**	LOI	Cl
IOW (wt%)	0.009	0.041	0.065	0.005	0.293	0.07	0.014	0.011	-	-	1.16	11.63	0.692

Table 2. Chemical composition of the prepared magnetic glass ceramics

Chemical Composition wt%	**Fe_2O_{3tot}**	**SiO_2**	**TiO_2**	**ZnO**	**Al_2O_3**	**MgO**	**CaO**	**Na_2O**	**K2O**	**ZrO_2**	**PbO**
IOH	74.71	16.92	0.311	0.046	3.1	0.3444	4.41	1.7	0.3114	0.0122	0.01
Chemical Composition wt%	**P_2O_5**	**CuO**	**Cr_2O_3**	**MnO**	**B_2O_5**	**BaO**	**V_2O_5**	**Ni_2O**	**SrO**		
IOH	0.54	0.012	0.031	1.39	27.33	72.4	0.078	0.073	0.0156		

2. 2 Preparation of the magnetic glass ceramic nanoparticles (MGNPS)

To produce magnetic nanoparticles, the heat treated IOH sample was used. Desktop high speed vibrating ball mill was used to carry out the high energy ball milling process at room temperature. One end of the principal axis of the mill connected with an eccentric wheel that has some certain angle degree with the principal axis, and the eccentric wheel is connected with the foundation of the ball mill through a tensile spring. When the electric machinery is in high speed operation, the eccentric wheel will swing at a high speed due to the tension of the spring. With the powerful vibration generated by the high speed swinging of the eccentric wheel, the ball milling jars fixed on the eccentric wheel also rotate and vibrate in a high – speed manner of 1200 rpm. Zirconium oxide jar was used and a vacuum stainless steel cover was used to operate the milling process in vacuum environment. Granularity of the material fed to the jar was less than 1mm and the maximum material loading was two thirds of the cubage of the ball milling jar (including milling balls). Two Zirconium oxide balls of 20 mm diameter were used in milling process. After the selected times (1, 3 and 5 h), the milling was stopped in order to prevent overheating and rapid engine wear, in addition, to collect the samples

2.3 water treatment experiments

The MB and CR solution was made up in stock solution of concentration 1000 (ppm) and was subsequently diluted to required concentrations using distilled water. Standard solutions of MB and CR were made up using distilled water as a solvent. Dilutions of concentrated samples were undertaken in order that the reduced optical density as found from the Spectrophotometer was in the range 0.001 to 0.6; it was found that more accurate results were obtained in this range. Then by multiplying these reduced optical densities by their dilution factor, the optical density of the original stock solution was obtained. All tests were carried out at room temperature (25±2°C) to eliminate any temperature effects, unless otherwise stated.

The calibration curves for both MB and CR were prepared by recording the absorbance (optical density) values for a range of known concentrations of dye solution at the wave length for maximum optical density (λ_{max}). This value, λ_{max}, was found from a full scan of the MB and CR spectrum. The values of λ_{max}, were determined using a double beam UV-visible Spectrophotometer (T80 UV-VIS Spectrophotometer PG Instruments ltd), UK, and this value is (665 nm) for MB and (556nm) for CR was used in all subsequent investigations using a Spectrophotometer.

Optical density readings for various samples (Tables 3.1& 3.2) were compared with the calibration curve (Figures 3.2&3.3) and transformed into concentration (ppm) terms.

In accordance with the Beer-Lambert's law and using least-squares method applied to the straight lines the optical densities follows a linear relationships to concentration as follows:

1) For MB Dye Conc. = 4.405*abs
2) For CD Dye Conc. =34.483*abs
The correlation coefficients are0.9902 and0.9986 for CR and MB, respectively

Table 3. Calibration curve for MB

Conc. (ppm)	0	1	1.5	2	2.5	3
Abs	0	0.224	0.322	0.503	0.565	0.666

Table 4. Calibration curve for CR

Conc.(ppm)	0	1	2	5	10	15
Abs	0	0.052	0.062	0.144	0.303	0.453

2.4 Characterization
The morphological study for the precursor hard magnetic glass ceramic sample and for the nanoparticles was carried out by using scanning electron microscope (SEM, FEI Quanta 200 Environmental Scanning Electron Microscope) and transmission electron microscope (TEM 2010).For TEM imaging, applying usual preparation methodology on the ball milled samples under investigation resulted in not evenly distributed particles on the form var grid but rather were on the grid bars therefore unobservable in the TEM. For successful imaging under the TEM, freeze-drying technique has been used to improve the long-term stability of the colloidal nanoparticles. The process of water removal from frozen samples by sublimation and desorption under vacuum is known as freeze-drying or lyophilization, this process can be controlled to reach a shelf life of several years.

SDTQ600 differential thermal analysis (DTA) instrument under inert gas was used to determine the thermal properties of the glass samples. Alumina was the inert reference material and 10°C/min was the used heating rate. DTA results were the guide to determine the heat-treatment temperatures needed to induce samples crystallization. To determine samples content and precipitated crystalline phases, X-ray diffraction using Ni-filled Cu Kα radiation was performed to samples before and after heat treatment. Bruker D8, an advanced X-ray diffraction instrument was used. ASTM x-ray diffraction card files were used for the interpretation of the XRD patterns of the reference data. Raman spectroscope (Model: Horiba Jobin Yvon Lab Ram ARAMIS) has been used to characterize the magnetic nanoparticles. Vibrating sample magnetometer (Quantum Design(R), Magnetic Property Measurement System (MPMS), SQUID VSM) was used to determine the magnetic properties of the magnetic nanoparticles and the precursor hard magnetic glass ceramic samples.

A double beam UV-visible Spectrophotometer (T80 UV-VIS Spectrophotometer PG Instruments ltd), was used for water treatment determination.

3 Results and discussions

Figure 1 illustrates the differential thermal analysis (DTA) of the prepared IOH sample before heat treatment. It revealed one endothermic peak at 554^{o}C followed by one exothermic peak at 716°C. The

endothermic effect mean increase in heat capacity, which cased due to transformation of glass from rigid to plastic structure resulted in the endothermic effect at ~ 554^{o}C **[26].** However, the exothermic peak is due to the crystallization effects, which is accompanied by releasing heat due to its lower free energy, reaches its maximum rate near the summit of the exothermal peak. The higher the intensity and sharpness of the exothermic peak is, the higher the propensity, velocity and bulk (internal) crystallization. In our case the exothermic peak is corresponding to the crystallization of Ba-hexaferrite crystallization as will be certified later by XRD. The broadness of the exothermic peak is due to surface crystallization or hardness to crystallize.

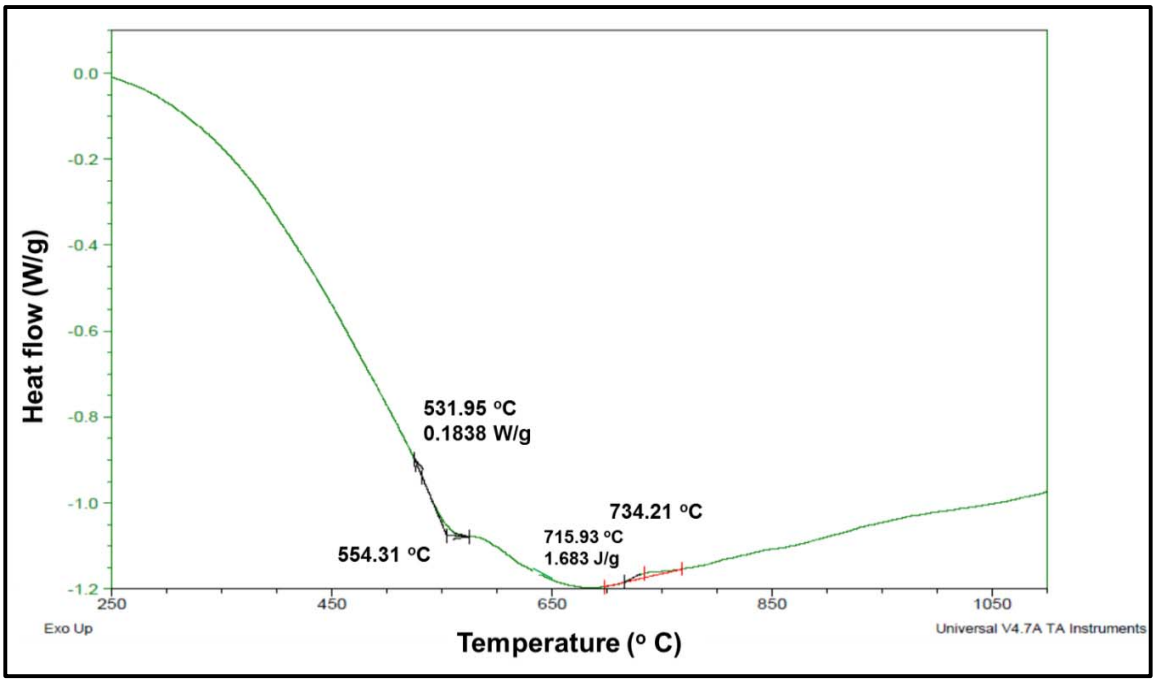

Figure 1. DTA scan for the as prepared IOH sample.

Figure 2. depict XRD analysis for unmodified iron ore waste (IOW) and the modified glass sample (IOH) before and after heat treatment. Heat treatment at 900^{o}C / 2 h was applied to the as quenched sample to convert it from glassy to crystalline structure. Un modified IOW revealed presence of hematite (Fe_2O_3), goethite FeO (OH) and wuestite ($Fe_{0.925}O$) phases as indexed in ASTM cards Nos89-0599,81-0464 and 89-686 respectively. On the other hands glass sample before heat treatment revealed amorphous structure, where hump at 2-theta 20 and 40° where appeared, no narrow XRD peaks were detected. Applying heat treatment at 900^{o}C/2 h revealed crystallization of pure Ba-hexaferrite ($BaFe_{12}O_{19}$); where XRD peaks were matched well with ASTM card No84-0757. This results evidence the success of the design composition to get pure Ba- hexaferrite.

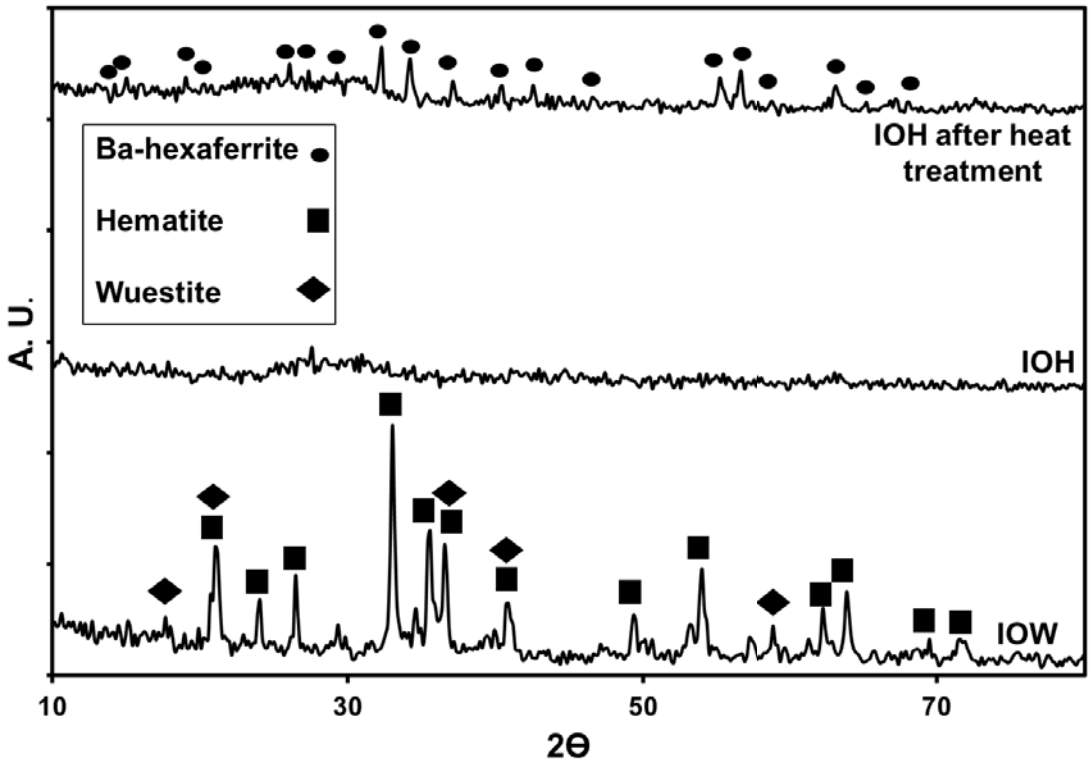

Figure 2. XRD spectra of IOW and IOH before and after heat treatment.

The comparative SEM images of the hand milled and high energy milled for 5h, at the same magnification for hard magnetic glass ceramics were shown in figure 3. (a, b). The hand milled samples are irregular with a rough surface, and the particles have a non-uniform distribution figure.3a. On the other hands, the mechanical milled revealed uniform distribution of very fine particles figure.3b; this confirms the effective conversion to magnetic nanoparticles during the 5 h high energy ball milling process. TEM of sample after high energy milled for 5h figure.3c revealed distribution of highly uniform agglomerated nanoparticles. The inherently large surface energy (> 100 dyn. cm-1) caused by the high surface area to volume ratio [27], in addition to strong magnetic dipole-dipole interactions and van der waals between particles are the reasons for agglomeration tendency of iron oxide nanoparticles [28]. After 5h milling duration the powder particles average size reached 26 nm. At lower temperature, the high reactivity of the 5 h-milled powders can facilitate densification and homogenization of the glass ceramics. This clarifies the reason of apparent agglomeration of the 5-h milled powder.

Figure 4. demonstrates the Raman spectra of heat treated IOH sample hand milled before and after 5 hours milling time. The fundamental Raman scattering peaks for $BaFe_{12}O_{19}$ observed at 686cm^{-1}, 615cm^{-1} refering to A_{1g} vibrations of Fe-O bonds at the bipyramidal 2b, octahedral $4f_2$, 2a+12k, 12k dominated and 2a sites respectively.The peak at 507cm^{-1} is due to E_{1g} vibrations, whereas the peak observed at 339 cm^{-1} is due to the E_{2g} vibration modes. The peak at 186 cm^{-1} originates from E_{1g} vibrations of the entire spinel block [29]. The particles after 5 hours milling time have the same characteristic peaks as the hand milled

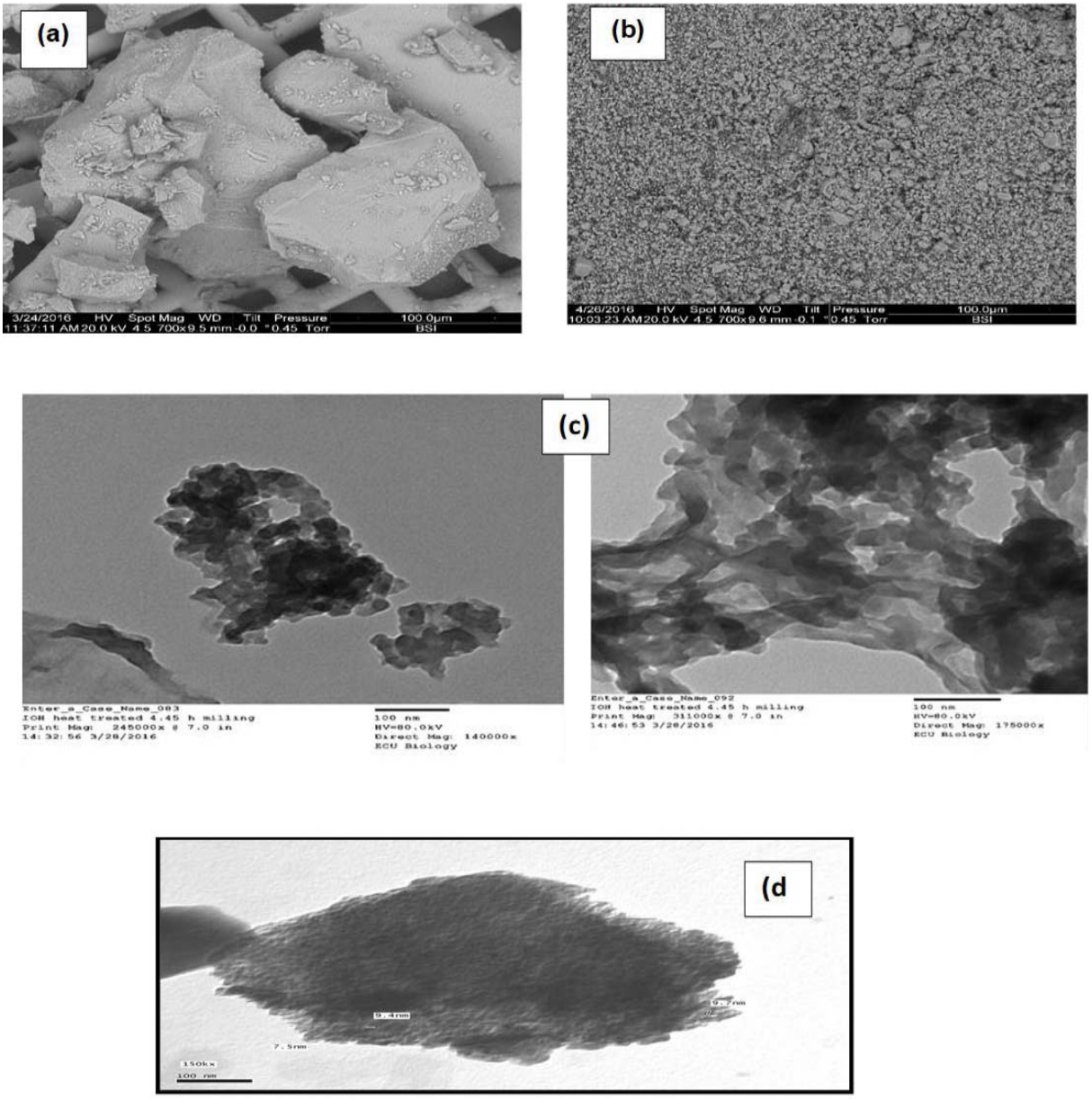

Figure 3. SEM images of (a) Hand milled and (b) 5 h milled IOH (700 x) magnification, (c, d) TEM images of 5 h milled IOH with 14000 X magnification compared to TEM image of (d) the hand milled heat treated IOH sample (150000x).

magnetic glass ceramic.The distortion of Ba-hexaferrite crystals due to milling process can be the reason of peaks intensity variation [30]. Intense peaks can be considered an indication of high degree of

crystallinity of nanoparticles, in addition, defects such as spin glass structures formation, BaO presence, cation redistribution and surface spins existence [31]. Increasing fractured particles percentage, higher aspect ratios for longer milling time or the formation of most of the nanoparticles rather than the disordered boundary regions with increasing milling time can lead to decrease in peaks intensity [32].

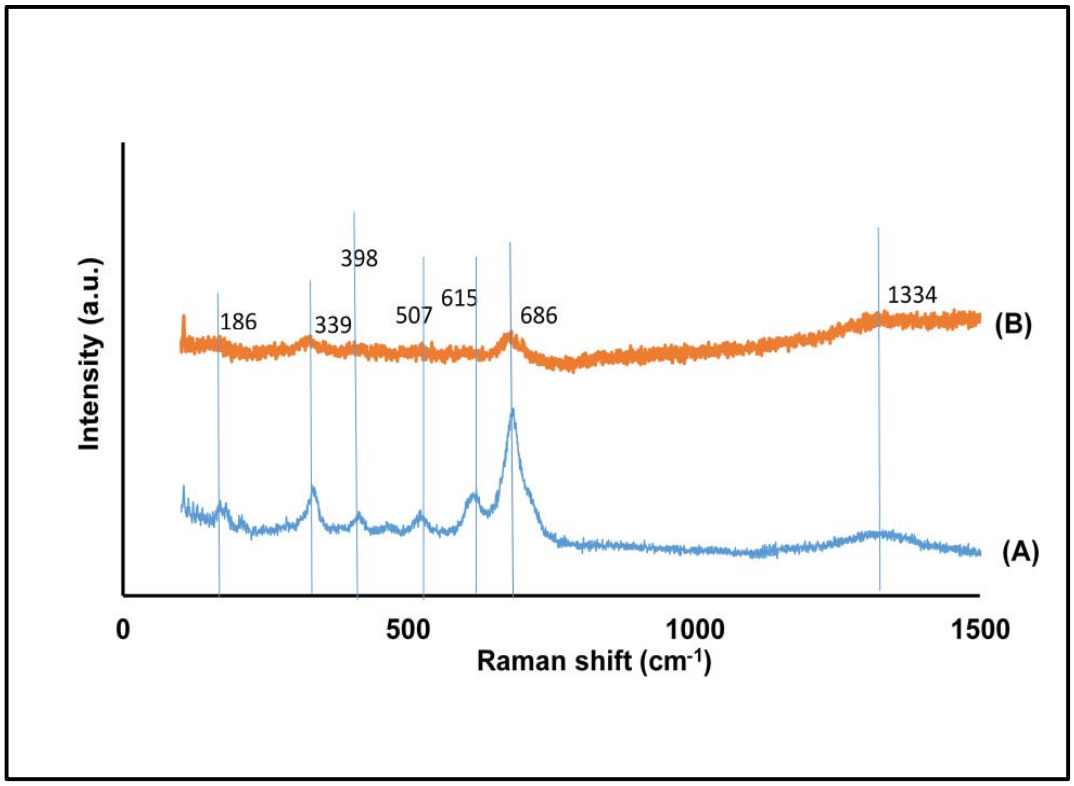

Figure 4. Raman spectra of (A) Hand milled and (B) 5hrs milled particles

Figure 5. Shows the room temperature magnetic hysteresis (*M-H*) loops of hand milled IOH and after 1, 3 and 5 hours milling time under a magnetic field strength of 20 KOe. Table 5 displays the relevant magnetic parameters: saturation magnetization (Ms), remanence (*Mr*), Coercivity (*Hc*) and *Mr/Ms* ratio obtained from M-H loops. In general, the magnetic field necessary to saturate the samples increases as the Ba-hexaferrite crystallization increases. As expected, saturation magnetization is due to crystallization of Ba-hexaferrite. It should be considered that Ba-hexaferrite is a ferromagnetic phase and amorphous glass matrix is an antiferromagnetic material with a very low saturation magnetization. As a consequence, the quantity of Ba-hexaferrite crystals present in the glass ceramic samples can be followed up by the variation of the saturation magnetization [30]. It is noticed that, *Ms* decreased by increasing milling time to reach 21.18 emu/g after 5 hours milling. The coercivity decreased from 1306Oe for hand milled sample to 83Oe after 1 hour milling and after that kept increasing by increasing milling time to reach the maximum value 1550Oe after 5 hours milling. Grain size, defects presence, strains, magneto-crystalline anisotropy, shape anisotropy and surface disorder usually affect the coercivity [31], [33].

The continual ball collisions with high energy in ball milling process is responsible primarily for the defects and strain resulted as well as the difference in magnetic properties of IOH powder after different milling time .

In the hand milling process, the reactants were in the interaction region of the mortar and pestle, can be ground to a limited extent. In the planetary ball milling process, almost all of the reactants are in the interaction region of the balls so that they can be simultaneously ground. The strains and defects generated by the repeated high energy ball collisions are still abound in the products. These findings explain the increase in H_c by increasing milling time (table 5).It can be observed from the loops that *Mr/Ms* values increased from 8.89 for the hand milled to 9.32 after 5 h milling. The remanence ratio enhancement were due to the increasing percentage of fractured particles and the formation of most of the nanoparticles with increasing milling time [32].These results consistent with Raman spectroscopy results. The magnetic properties results confirm that after milling process, the material is still strongly magnetic and enable magnetic manipulation and recovery of the sorbent in the water treatment as shown in inset in figure 5.

Table 5. Magnetic properties of 1- hand milled, 2- 1hr, 3- 3hrs, and 4- 5 hrs milling particles.

Sample	Ms (emu/g)	Mr (emu/g)	Hc (Oe)	Mr/Ms
Hand milled	22.56	8.89	1306	0.39
5 hrs milled particles	21.18	9.32	1550	0.44

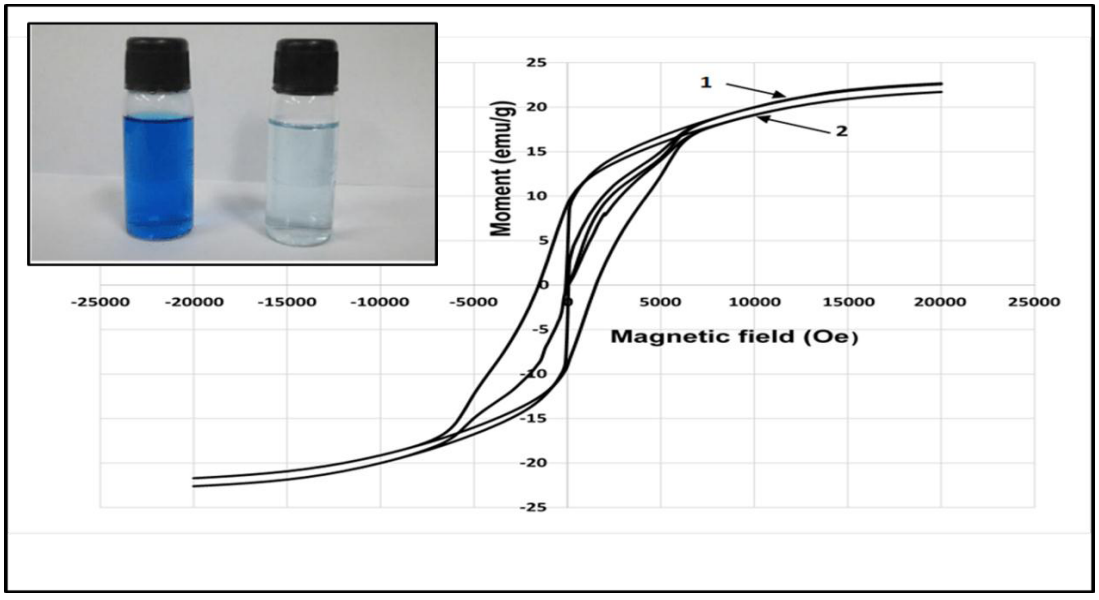

Figure 5. Room temperature M-H hysteresis loops for 1- Hand milled 2-5hrs milled IOH particles.

The presence of organic pollutants in the water resources is a major risk to the human health and ecosystem. Therefore, an effective low cost adsorbent with high adsorption capacity for organic pollutants removal is desirable. Many researchers studied the organic contaminants adsorption using iron oxide nano-material as, particularly for the efficient treatment of large-volume water samples and fast separation by employing a strong external magnetic field.

In this study, Methylene blue (MB) and Congored (CR) as common dyes in many industries were selected. These dyes were used for studying the removal capacity of the hand milled and the 5 hrs. milled magnetic nanoparticles. A constant mass of the hand milled and 5 hours milled particles were added to 100 ml (cm^3) bottles containing 50 ml of solution. The bottles were sealed together with appropriate blanks and mechanically shacked in a constant temperature, constant agitation shaker bath for a period of 3-h was used. The speed of agitation was kept constant for each run throughout the experiments to ensure equal mixing. After that time, the samples were centrifuged at 5000 rpm for 30 min. to separate the magnetic particles. The adsorption isotherm calculation was important to describe the interaction mechanism between adsorbate and adsorbent and to show the adsorption capacity of adsorbent. The amount of dye adsorbed is calculated from the following equation

$$qe = \frac{(Co - Ce)V}{m}$$

Where qe is the equilibrium adsorbent capacity (mg/g), Co and Ce are the initial and final dye concentration (mg/l) respectively, V is the volume of dye solution and m is the mass of adsorbent (g).

Figures 6. shows the effect of contact time on the adsorption of Methylene blue (MB) dye by 5 hrs. milled nanoparticles compared to the hand milled particles. The equilibrium concentration for MB on the hand milled particles reached after 25 min. Adsorption of dye was quit rapid initially and the rate of adsorption became slower with time and reached constant value (equilibrium time). The initial faster rate may be due to the availability of uncovered surface area of the adsorbent [37]. For MB dye, the adsorption capacity of the 5 hours milled magnetic particles is 200 mg/g while it is 166.5 mg/g for the hand milled particles. Similarly, for CR dye, the adsorption capacity of the 5 hours milled nanoparticles is 124.5 mg/g while it's 104 mg/g for the hand milled magnetic particles. The fast removal rate is mainly attributed to the electrostatic attraction between the surface of the particles and the MB and CR dyes in the solution and the nanostructure with high surface area.

Table 6. A comparison of the adsorption capacities of the nano-sorbent used by present study and selected studies.

Group	Nanosorbents	Dye	Adsorption capacity	Reference
Ying Qi Wang et al.	$MnFe_2O_4$	Congo red	39.3 mg/g	[34]
Kah Aik Tan et al.	Fe_3O_4-MCP	Methylene blue	24.4 mg/g	[35]
Saksornchai et al.	CTAB coated Fe_3O_4	Congo red	93.5 mg/g	[36]
This study	$BaFe_{12}O_{19}$	Methylene blue Congo red	200 mg/g 124.5 mg/g	

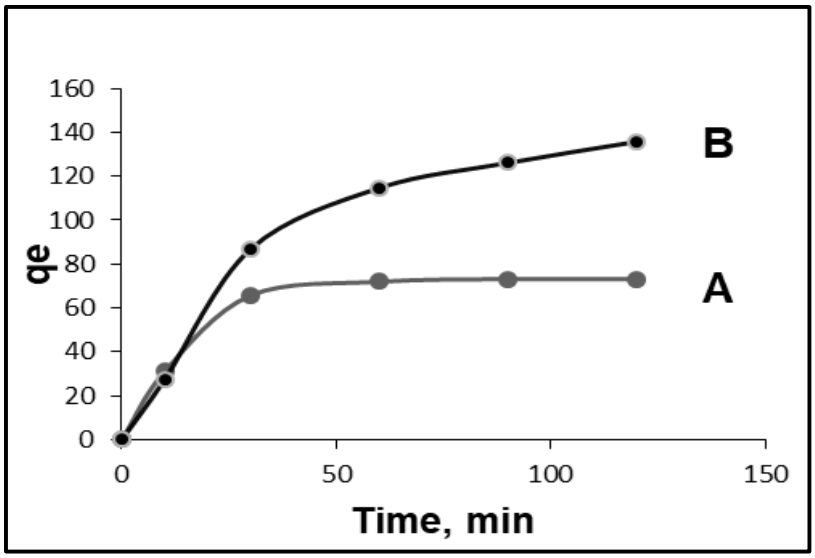

Figure 6. Effect of contact time on removal of methylene blue dye using A, Hand milled and B, 5 hrs milled particles.

Similar to heavy metal adsorption, the adsorption of organic contaminants take place by surface exchange reactions until the surface functional sites are fully occupied then contaminants could diffuse into the adsorbent for further interactions with the functional groups [38-40]. The nanostructured materials with high surface area increase the contact between the dye and the adsorbent surface. It is apparent that the adsorption capacity of the $BaFe_{12}O_{19}$ nanoparticles prepared in this study is higher than that obtained previously by other workers (table 6). This confirms that the recycled magnetic nanoparticles could be a promising adsorbent for waste water treatment.

4 Conclusions

1-Hard ferromagnetic glass-ceramics were prepared by recycling Baharaya oasis iron ore waste.

2-XRD data confirmed that, the heat treatment schedule (900oC/ 2h) chosen according to DTA results had a positive effect on Ba-hexaferrite crystallization.

3-By using mechanical milling technique, uniformly distributed hard ferromagnetic glass-ceramics with 26 nm particle size has been obtained after 5 h milling time.

4-Raman spectroscopy analysis confirmed that, the produced nanoparticles after 5 hours milling time have the same characteristic peaks like the hand milled magnetic glass ceramic precursor.

5-Saturation magnetization decreased by increasing milling time to reach 21.18 emu/g after 5 hours milling. The coercivity decreased from 1306 Oe for hand milled sample to 83 Oe after 1 hour milling and after that kept increasing by increasing milling time to reach the maximum value 1550 Oe after 5 hours.

6-Increasing percentage of fractured particles and higher aspect ratios for longer milling time explain the remanence ratio enhancement after 5 hours milling.

7- Reducing particle size increased the adsorption capacity of the magnetic particles. For MB dye, the adsorption capacity of the 5 hrs milled magnetic particles is 200 mg/g while it is 166.5 mg/g for the hand milled particles. For CR dye, the adsorption capacity of the 5 hrs milled nanoparticles is 124.5 mg/g while it's 104 mg/g for the hand milled magnetic particles.

5. References

[1] Aderhold J, Davydov V Yu, Fedler F, Klausing H, Mistele D, Rotter T, Semchinova O, Stemmer and Graul J 2001 J. Cryst. Growth 222 701
[2] S. A. M. Abdel-Hameed, A. M. El Kady, 2012. J. Adv. Mater. 3 167.
[3] Jason Hill, Erik Nelson, David Tilman, Stephen Polasky and Douglas Tiffany, 2006 Proceedings of the national academy of sciences of the United States of America 103 30.
[4] J. Smit and H.P.J. Wijn, 1959 New York, Wiley.
[5] G.Schmid,2004 Wiley-VCH, Wein-heim.
[6] K.J.Klabunde, 2001 Wiley-Interscience,New York.
[7] S.Sun, H.Zeng, D.B.Robinson, S.Raoux, P.M.Rice,S.X.Wang, 2003 Journal of the American chemical society, 126 273.
[8] Xiaoyan Zhang, Qiaoyu Dai, Xiaobin Huang and Xiaozhen Tang, 2009 Solid state sciences, 11 1861.
[9] Mani Diba, Qurania-MentiGoudouri, Felipe Tapia and Aldo R. Boccaccini, 2014 Journal of current openion in solid state and materials science 18 147.
[10] SeungyounLyu, Chunlan Huang, Hong Yang and Xinping Zhang, 2013 Journal of orthopedics research 31 1382.
[11] C. Feng, K. C. Khulbe, T. Matsuura, S.Taba and A. F. Ismail, 2013 Separation and purification technology 102 118.
[12] JeehyeByun, Hasmukh A. Patel and Cafer T. Yavuz, 2014 Journal of nanoparticles research 16 2787.
[13] S.C. Tjong, and H. Chen, 2004 Materials Science and Engineering, 45 1.
[14] J.S. Benjamin, 1990 Metal Powder Rep. 45 122.
[15] D.L. Zhang, 2004 Progress in Materials Science 49 537.
[16] T. S. Ward, W. Chen, M. Schoenitz, R. N. Dave, and E. Dreizin, 2005 ActaMaterialia, 53 2909
[17] Q.S. Mei, and K. Lu, 2007 Progress in Materials Science 52 1175.
[18] M. Sherif El-Eskandarany, K. Sumiyama, and K. Suzuki, 1997 ActaMateialia, 45 1175.
[19] S. Zghal, R. Twesten, F. Wu, and P. Bellon, 2002 ActaMaterialia, 50 4711.
[20] O. Ligrini, E. Oliveros, A. Braun, 1993 chem. Rev. 93 671.
[21] C. T. Helmes, C. C. Sigman, Z. A. Fund, M. K. Thompson, M. K. Voeltz, M. Makie, 1984 J. Environ. Sci. Health A. 19 97.
[22] M. Boeningo, 1994 Washington, DC: US Gov. printing off., DNHS (NIOSH), 80.
[23] R. Han, D.Ding, Y. Xu, W. Zou, 2008 Bioresour. Technol. 99 2938.
[24] V. S. Mane, P.V. Vijay Babu, 2011 Desalination 273 321.
[25] M. Ghaedi, M. N. Biyareh, S. N. Kokhdan, S. Shamsaldini, R. Sahraei, A. Daneshfar, S. Shahriyar, 2012 Mater. Sci. Eng., C 32 725.
[26] A. Afkhami, R. Moosavi, 2010 J. Hazard. Mater. 174 398.
[27] Salwa A.M. Abdel-Hameed , Mohamed A. Marzouk , Mohamed M. Farag, 2014 Journal of Advanced Research 5 543.
[28] C.Buzea, I.Pacheco, K.Robbie, 2007 Biointerphases 8630 MR 17
[29] DonyaRamimoghadam, Samira Bagheri and Sherifah Bee AbdHamid, 2015 Colloids and surfaces B:Biointerfaces 133 388.
[30] V. Rane, S. Meena, S. Gokhale, S. M. Yusuf, G. Phatak and S. Date, 2013 J. Electron. Mater.42 761.
[31] M. K. Roy, B. Haldar, H. C. Verma, 2006 Nanotechnology 17 232.
[32] S. Chkoundali, S. Ammar, N. Jouini, F. Fiévet, P. Molinié, M. Danot, F. Vallain, J. M. Grenèche, 2004 J. Phys.: Condens. Matter 16 4357.
[33] V. M. Chakka, B. Altuncevahir, Z. Q. Jin, Y. Li, and J. P. Liu, 2006 Journal of applied physics 99

08E912.
[34] A.B. Nawale, N. S. Kanhe, K. R. Patil, S. V. Bhoraskar, V. L. Mathe, A. K. Das, 2011 J. Alloy. Compd. 509 4404.
[35] Ying Qi Wng, RongMin Cheng, Zi Wen, and LiJun Zhao, 2011 Eur. J. Inorg.Chem. 2942.
[36] Kah Aik Tan, Norhashimah Morad, Tjoon Tow Teng, Ismail Norli and P. Panneerselvam, 2012 APCBEE Procedia 1 83
[37] Saksornchai E, Kavinchan J, Thongtem S, Thongtem T., 2018 Mat. Lett. 142 213
[38] Tayyebeh Madrakian, Abbas Afkhami, MazaherAhmadi, 2012 Spectrochimicaacta part a: molecular and biomolecular spectroscopy 99 102.
[39] Hu J, Shao DD, Chen CL, Sheng GD, Ren XM, Wang XK., 2011 J Hazard Mater 185 463.
[40] Ma ZY, Guan YP, Liu XQ, Liu HZ., 2005 J Appl Polym Sci 96 2174.
[41] Zhao XL, Wang JM, Wu FC, Wang T, Cai YQ, Shi YL, 2010 J Hazard Mater 173 102.